

Middle East Technical University  
Electrical and Electronics Engineering Department

# EE464 Hardware Project Simulation Report

Ecem KARAMERCAN 2304863

Tuğçe Şevval KAYA 2304921

Zehra GUNES 2232023

Zeynep COKLU 2231694

# Table of Contents

<b>1</b>	<b>Introduction</b>	<b>3</b>
1.1	Problem Statement . . . . .	3
1.2	Design Specifications . . . . .	3
<b>2</b>	<b>Topology Selection</b>	<b>5</b>
2.1	Linear Power Supplies . . . . .	5
2.2	Switching DC Power Supplies . . . . .	5
2.2.1	Flyback Converter . . . . .	5
2.2.2	Forward Converter . . . . .	6
2.2.3	Push-Pull Converter . . . . .	7
<b>3</b>	<b>Operating Mode Selection</b>	<b>9</b>
<b>4</b>	<b>Analytical Calculations</b>	<b>10</b>
<b>5</b>	<b>Computer Simulations</b>	<b>12</b>
5.1	Simulations in Simulink - Ideal Case . . . . .	12
5.1.1	Simulation Results for $V_{in}=24$ Volts . . . . .	13
5.1.2	Simulation Results for $V_{in} = 48 V$ . . . . .	16
5.2	Simulation in LTspice . . . . .	21
5.2.1	Controller Implementation . . . . .	21
5.2.2	Simulation Results . . . . .	27
<b>6</b>	<b>Magnetic Design</b>	<b>32</b>
6.1	Core Selection . . . . .	32
6.2	Cable Selection . . . . .	34
<b>7</b>	<b>Component Selection</b>	<b>37</b>
7.1	MOSFET Selection . . . . .	37
7.2	Diode Selection . . . . .	37
7.3	Output Capacitor Selection . . . . .	38
7.4	Controller Selection . . . . .	38
7.5	RCD Snubber Circuit Selection . . . . .	38



# Chapter 1

## Introduction

### 1.1 Problem Statement

Electrical connection between in the input and output side is known as a strong disadvantage in current technology since the grounded input is also presented in the output side. To solve this common problem, a transformer is provided as it is able to separate the output from the input side electrically so that an isolated DC stage is obtained. In this hardware project, the main objective is to design an isolated DC-DC converter with closed loop control mechanism.

### 1.2 Design Specifications

The given limitations and specifications are provided for this design as follows:

- Minimum Input Voltage: 24 V
- Maximum Input Voltage: 48 V
- Output Voltage: 15 V
- Output Power: 45 W
- Output Voltage Peak-to-Peak Ripple: %3
- Line Regulation(Deviation of percent output voltage when input voltage is changed from its minimum to maximum or vice versa): %3
- Load Regulation(Deviation of percent output voltage when load current is changed from %10 to %100 or vice versa): %3

Knowing all of these, the report consists of the following parts: a topology selection among the isolated converters was made considering their advantages and

disadvantages. Then, analytical calculations were provided based on the theoretical background of the topology. Deciding the values for the necessary parameters, the computer simulations were also given. The rest of the report contains the component selections including the magnetic design phase as well.

## Chapter 2

# Topology Selection

### 2.1 Linear Power Supplies

- Advantages
  1. Low electromagnetic emission problems occur.
  2. The transient response is at an advanced level.
- Disadvantages
  1. They have low frequency operation limits.
  2. BJT operates in linear region, causing extra heat dissipation.
  3. The efficiency is achieved at low level (%30 - %60 band).
  4. They can only step down the output voltage.

### 2.2 Switching DC Power Supplies

#### 2.2.1 Flyback Converter

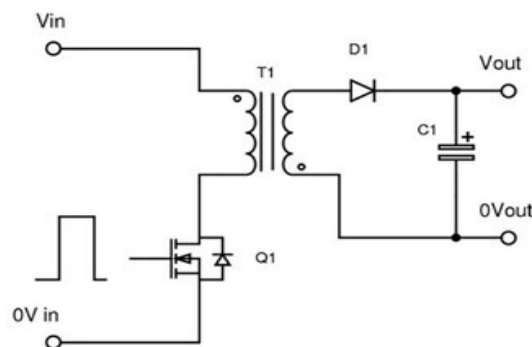


Figure 2.1: Flyback Converter Circuit Schematic

- Advantages

1. Fewer components are utilized to obtain a regulated output with respect to other switching DC power supplies. This enhances for a designer to have cost advantage and magnetic and electrical design simplicity.
2. By only a single control mechanism, the regulated output is achieved.
3. High voltage gain is possible to be achieved.
4. It can be chosen in low power applications such as TV or PC. Since given task in this project also demands low power (96 W), it can be an effective solution.

- Disadvantages

1. Energy storage is a must for the transformer. This limits the transformer design by ferrite or air gapped cores mostly.
2. It requires an additional snubber circuit if its advanced versions are not utilized (two transistor or parallel).
3. A pulsating current occurs at the output side due to lack of inductance.

### 2.2.2 Forward Converter

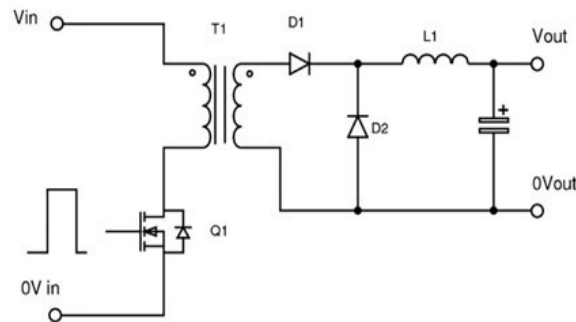


Figure 2.2: Forward Converter Circuit Schematic

- Advantages

1. The output inductor and diode ensure a continuous current flow in the output side.
2. The transformer is utilized as a direct power transfer tool, not to store.
3. Gapless cores can also be used leading higher  $L_m$  and fewer ripples.

- Disadvantages

1. The cost is increased with additional inductor and diode.
2. The voltage stress on the switch is higher, causing higher voltage range requirement for the switches.
3. Gain variety in DCM operation occurs at higher level.
4. Snubber circuit implementation is needed if its practical version is not used. If practical case is chosen, then this time more transformer windings, hence more complex magnetic design process are needed.

### 2.2.3 Push-Pull Converter

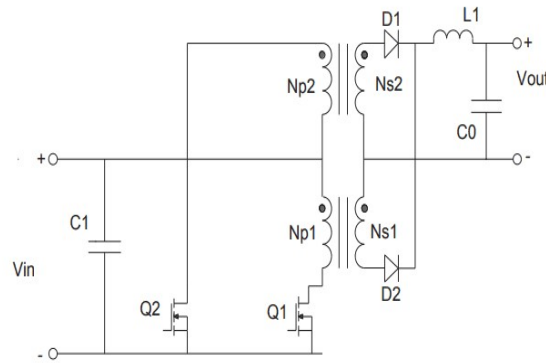


Figure 2.3: Push-Pull Converter Circuit Schematic

- Advantages

1. Utilization of the magnetic core is at more advanced stage since it can be operated not just at 1st but also in 3rd quadrant of B-H curve.
2. It can properly function even at high power applications.
3. Transformer rating required is usually smaller than Forward topology.
4. The output is obtained without a distortion.
5. DC components of the output currents at two consecutive switching periods magnetically oppose each other and the core saturation risk is reduced.

- Disadvantages

1. The switching mechanism is more complex with respect to other topologies since it requires two switches and forbids turning on simultaneously for the switches.



2. The cost is increased as it needs more transformer windings and switches compared to the Flyback topology especially.
3. It needs longer and more detailed magnetic design phase due to increased number of transformer windings compared to both Flyback and Forward topologies.

Considering the given criteria, budget, magnetic design phase and provided duration for the project, the team has decided on to design **Flyback topology** as it has the advantages for the costs (requiring fewer components) and a simpler form with respect to other ones (only one switch to regulate, no inductor takes place at the output side: reduced duration and more flexibility on the magnetic design phase)

## Chapter 3

# Operating Mode Selection

The flyback converter can work in three ways: continuous, discontinuous conduction and critical conduction mode. All operation modes have advantages and disadvantages. Generally, the applications with low power, the discontinuous conduction mode is more preferable. On the other hand, the CCM is usually chosen for high power and low input cases. In discontinuous mode, inductor charges and discharges completely, hence the current ripple could be higher than continuous current mode. Also, EMI problems are lower in CCM mode. The controller selection for determining operation mode is crucial. It might be hard to find suitable controller for the operation type. Therefore, the controller selection is discussed in details in Chapter 6. We decided to operate in continuous conduction mode, its advantages are more useful for this application. One of the main reasons of that decision is controller implementation. It is harder to operate converter in critical conduction mode, also it is harder to control. Therefore, CCM is selected for operation mode.

## Chapter 4

# Analytical Calculations

In this part, analytical calculations of the flyback converter are made for the ideal case. According to the research, the duty cycle of the flyback converter should be lower than 0.5 to diminish output ripple, also we made sure of the proper operation of the switch. Therefore, we have decided the turn ratio( $N_1/N_2$ ) as 1.33 so that the duty cycle is changing between %29.36-%45.39.

The controller operates flyback in continuous current mode. All calculations are made assuming continuous current operation. We have taken boundary mode results as the limit values for continuous conduction. Therefore, continuous current mode formulas are utilized for boundary condition calculations.

- Duty Cycle Calculation

$$V_{out} = V_{in} \left( \frac{D}{1-D} \right) \left( \frac{N_2}{N_1} \right)$$

for  $V_{out} = 15V$ , &  $\frac{N_2}{N_1} = 0.75$  when  $V_{in} = 24V$

$$D_{max} \cong 0.45$$

when  $V_{in} = 48V$

$$D_{min} \cong 0.29$$

The maximum required inductance can be calculated as follows [1]

$$L_m = \frac{V_{in}^2 \eta}{K_L P_o f_s} \frac{V_{out}^2 N_{ps}^2}{(V_{in} + V_{out} N_{ps})}$$

Setting the magnetizing inductor current as:

$$\Delta I_{Lm} = K_L I_{Lm}$$

where

- $K_L$  is the fraction chosen, we have chosen  $K_L$  as 2 in order to set boundary operation.
- $N_{ps} = \frac{N_1}{N_2} = 1.33$
- $f_s = 70kHz$
- $\eta = 1$  (ideal case)

Then, minimum magnetizing inductance is determined when  $V_{in} = 48V$ .

$$L_{m_{max}} = 31.6 \mu H$$

- Calculation of maximum voltages on diode and MOSFET,

$$V_{sw_{max}} = V_{in_{max}} + V_{out}N_{ps} = 67.95V$$

$$V_{d_{max}} = V_{in_{max}}N_{sp} + V_{out} = 51V$$

Generally in applications, rated voltage of MOSFETs are chosen as 1.7 multiplication of maximum voltage while 1.5 multiple of maximum value in diodes,

$$V_{sw_{rated}} \geq 118.915V$$

$$V_{d_{rated}} \geq 76.5V$$

- Output capacitance calculation

$$\Delta V_{out} = \Delta Q C = \frac{V_{out} D_{max} T_s}{RC}$$

The output voltage ripple constraint is  $\frac{\Delta V_{out}}{V_{out}} \leq 0.03$ . Then, the required capacitance is:

$$C \geq 42.85 \mu F$$

Choosing

$$C = 50 \mu F \text{ and } \Delta V_{out} = 0.386V$$

The ripple voltage at the output also can be calculated by adding ESR value of capacitance. The voltage ripple with ESR is equal approximately two times of ripple without ESR. Therefore:

$$\Delta V_{out,ESR} = I_{Lm_{max}} \frac{N_1}{N_2} r_c \leq 0.06 \text{ and } r_c \leq 7.9 m\Omega$$

## Chapter 5

# Computer Simulations

### 5.1 Simulations in Simulink - Ideal Case

According to calculated values, the circuit schematic in Simulink is constructed as can be seen from Figure 5.1.

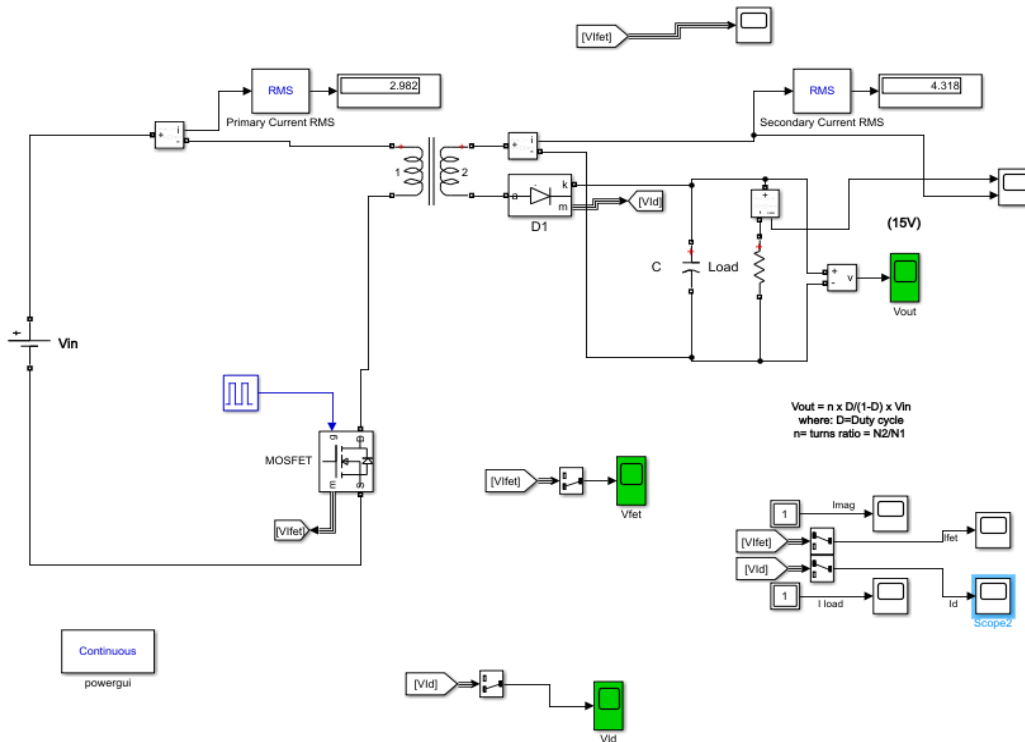


Figure 5.1: Flyback Converter Circuit Schematic in Simulink

The simulations are made for two cases: first one for minimum input voltage  $V_{in} = 24 V$  and second one for maximum input voltage  $V_{in} = 48 V$ . The transformer turn ratio and magnetizing inductance is given in Figure 5.2 as calculated. The non-

idealities are not considered for this simulation.

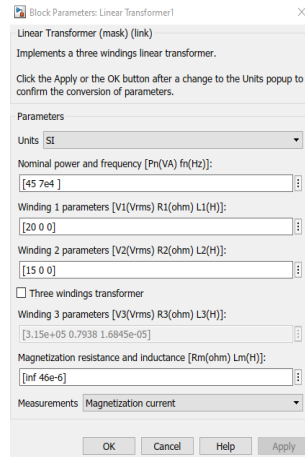
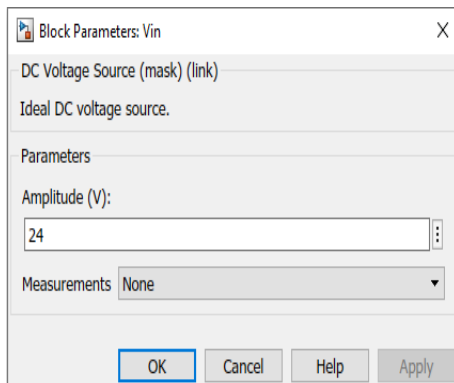


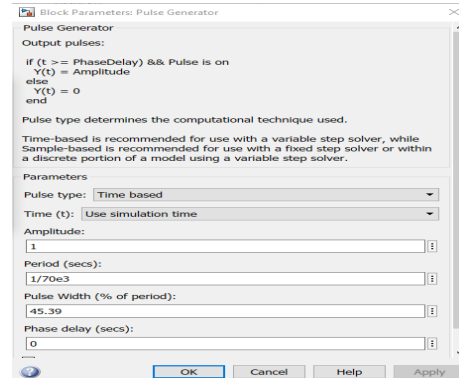
Figure 5.2: Transformer Properties

### 5.1.1 Simulation Results for $V_{in}=24$ Volts

For  $V_{in} = 24V$ , the duty cycle that is required to applied is calculated as %45.39.



(a) The Minimum Input Voltage



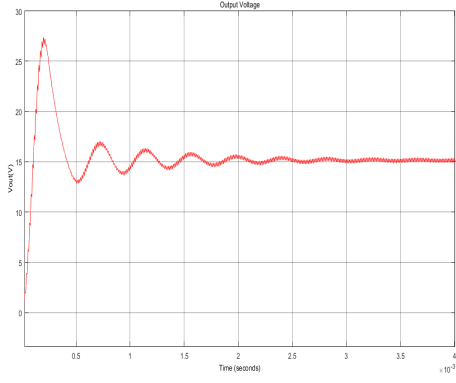
(b) The Maximum Duty Cycle for Minimum Input Voltage

Figure 5.3: The Minimum Input Voltage Simulation Properties

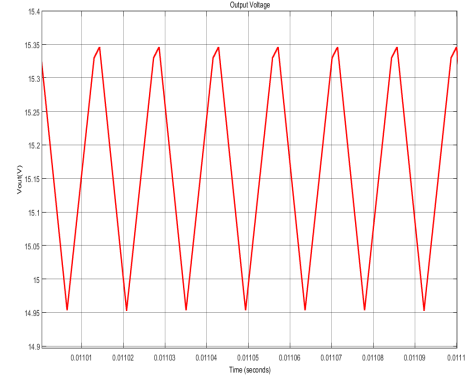
The output voltage waveforms for both transient and steady state is given in Figures 5.4.

As can be seen from Figure 5.4, the output voltage ripple is roughly equal to 0.4 V, therefore this is satisfied the design consideration.

The output current waveform for transient and steady state is given in Figure 5.5 respectively.

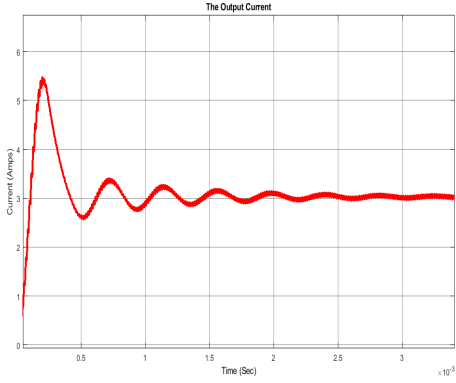


(a) Transient

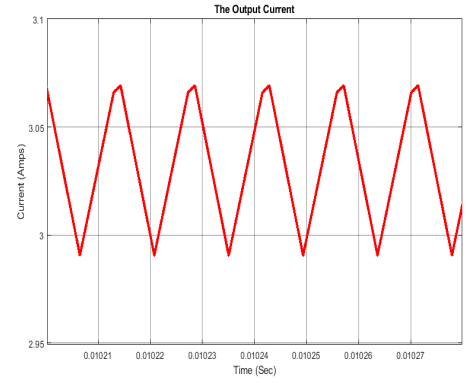


(b) Steady State

Figure 5.4: The Output Voltage for  $V_{in} = 24\text{ V}$



(a) Transient



(b) Steady State

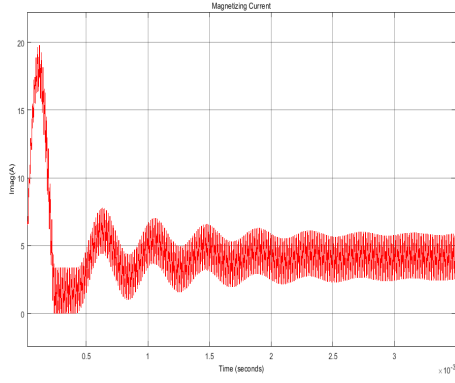
Figure 5.5: The Output Current for  $V_{in} = 24\text{ V}$

The primary energy storage component is magnetizing inductance of the transformer. Therefore, the magnetizing current at this inductance is critical. Previously, the operation mode is chosen as continuous conduction mode so the current cannot reach the zero while operating. The transient and steady state waveforms are given in Figure 5.6. As expected, the flyback converter operates at CCM.

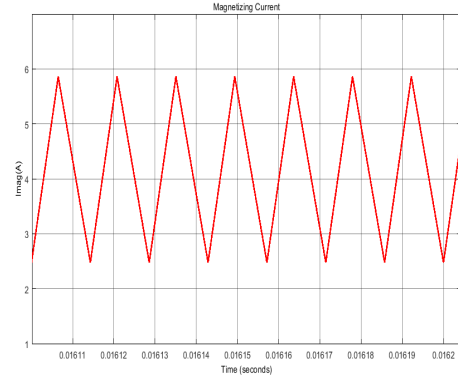
The transient voltage and current of MOSFET and diode are crucial for component selection. Especially, the maximum voltage of these semiconductors should be considered for component selection. The controller is also effective on which MOSFET should be used.

The current of MOSFET at transient and steady state is shown in Figure 5.8.

Therefore, the maximum voltage and current are known for switch for minimum input.

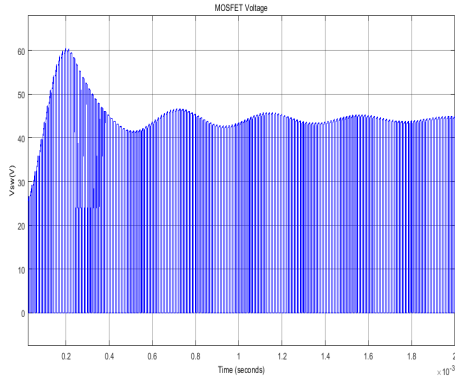


(a) Transient

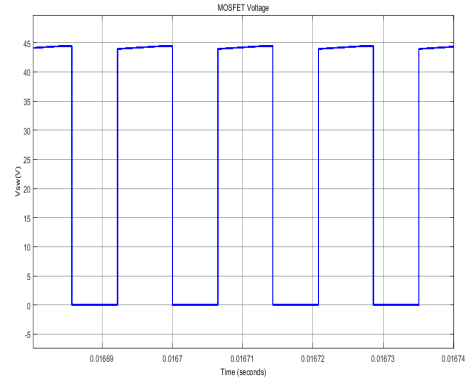


(b) Steady State

Figure 5.6: The Magnetizing Current for  $V_{in} = 24\text{ V}$

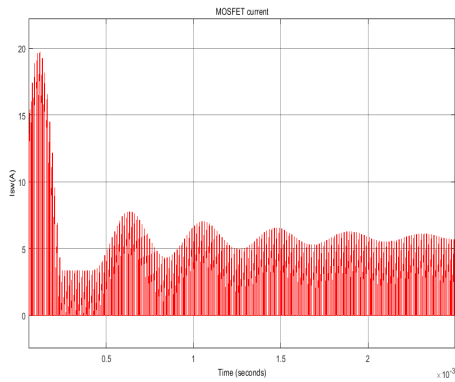


(a) Transient

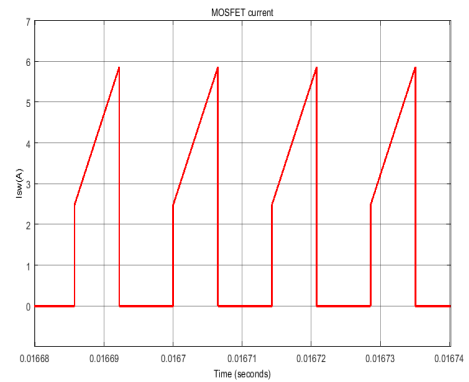


(b) Steady State

Figure 5.7: MOSFET Voltage at Transient and Steady State for  $V_{in} = 24\text{ V}$



(a) Transient



(b) Steady State

Figure 5.8: MOSFET Current at Transient and Steady State for  $V_{in} = 24\text{ V}$



The transient and steady state voltage waveforms of the diode are given in Figure 5.9.

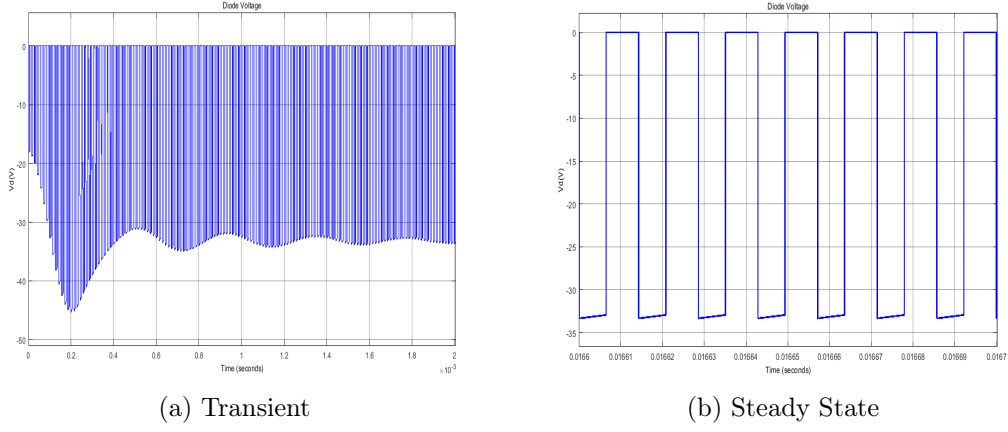


Figure 5.9: Diode Voltage at Transient and Steady State for  $V_{in} = 24\text{ V}$

The transient and steady state current waveforms of the diode are given in Figure 5.10.

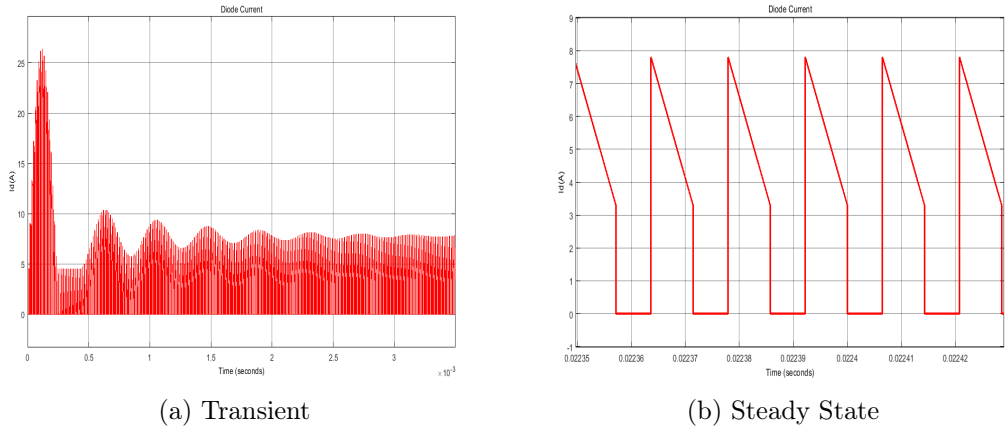
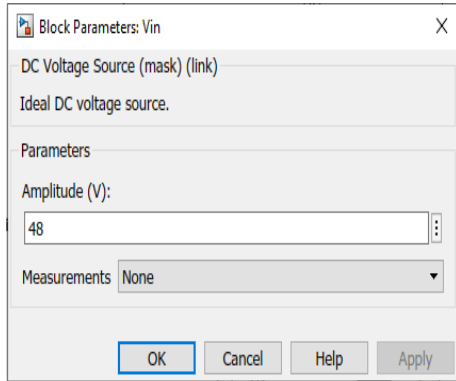


Figure 5.10: Diode Current at Transient and Steady State for  $V_{in} = 24\text{ V}$

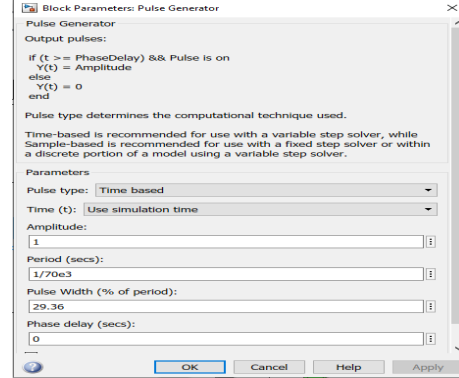
### 5.1.2 Simulation Results for $V_{in} = 48\text{ V}$

Now, the input voltage is applied 48 Volts which the maximum input. The duty cycle that is required for the maximum input is calculated as %29.36.

At transient and steady state the output voltage for  $V_{in} = 48\text{ V}$  is given in Figure 5.12.

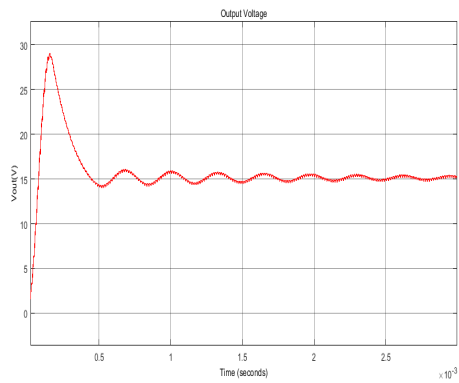


(a) The Maximum Input Voltage

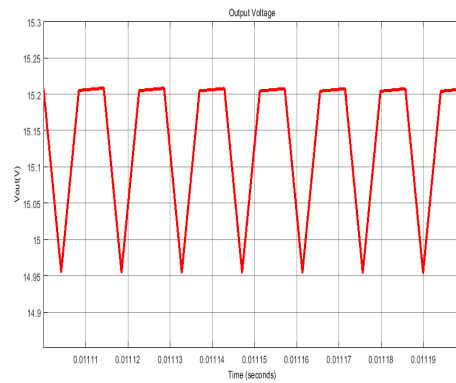


(b) The Minimum Duty Cycle for Maximum Input Voltage

Figure 5.11: The Maximum Input Voltage Simulation Properties



(a) Transient



(b) Steady State

Figure 5.12: The Output Voltage for  $V_{in} = 48 V$

Figure 5.12 is shown the output voltage ripple is smaller than the design consideration. Moreover, the output capacitance might be selected a lower value than the simulation value. Since, the cutting edges are observed at the peak points of the waveform.

The output current at transient and steady state is given in Figure 5.13. As can be seen the output current ripple is roughly zero.

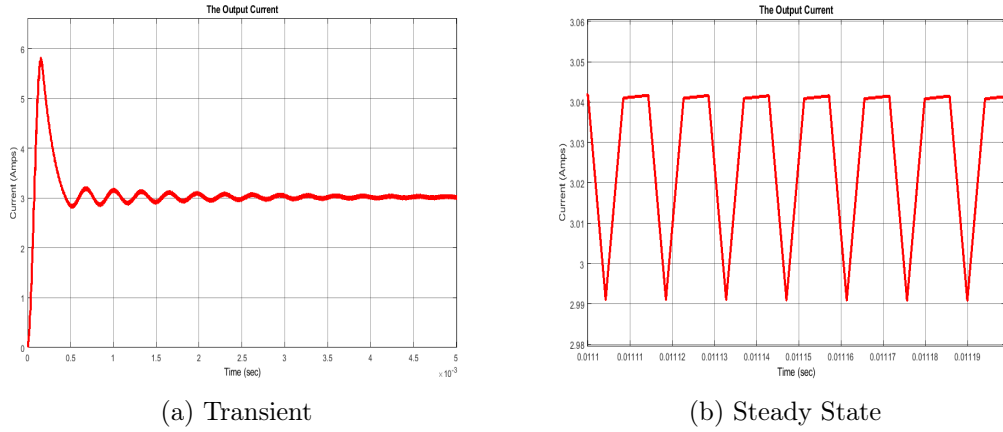


Figure 5.13: The Output Current for  $V_{in} = 48\text{ V}$

The magnetizing current of transformer at transient and steady state is given in Figure 5.13.

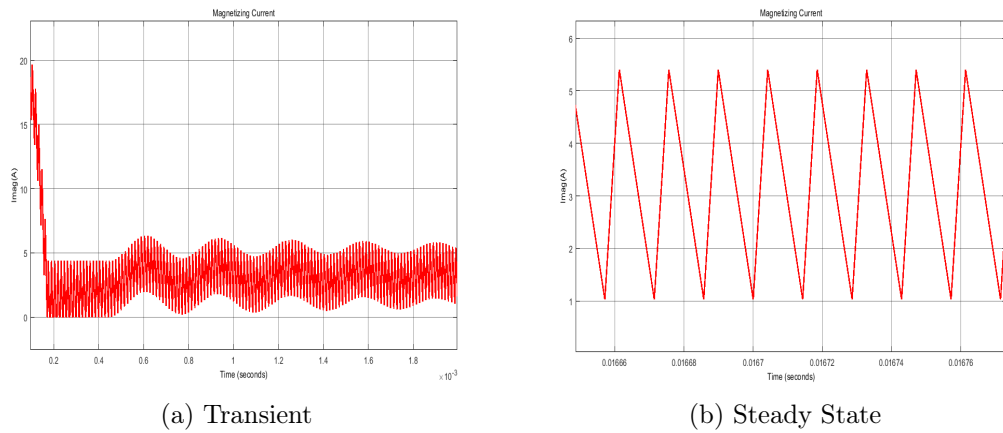


Figure 5.14: The Magnetizing Current for  $V_{in} = 48\text{ V}$

Figure 5.15 is shown MOSFET voltage at transient and steady state when the maximum input is applied.

As shown in Figure 5.15, the maximum voltage at MOSFET is approximately 90

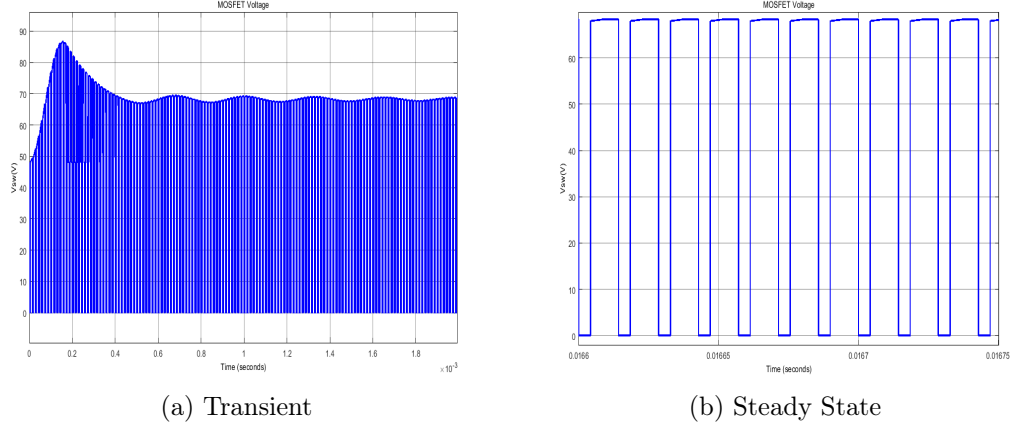


Figure 5.15: MOSFET Voltage at Transient and Steady State for  $V_{in} = 48\text{ V}$

Volts which is similar to analytical calculations. This value is the maximum voltage at switch during operation. Therefore, it should be considered for switch selection. It will be discussed in component selection chapter.

The current waveforms of MOSFET for maximum input voltage is given in Figure 5.16.

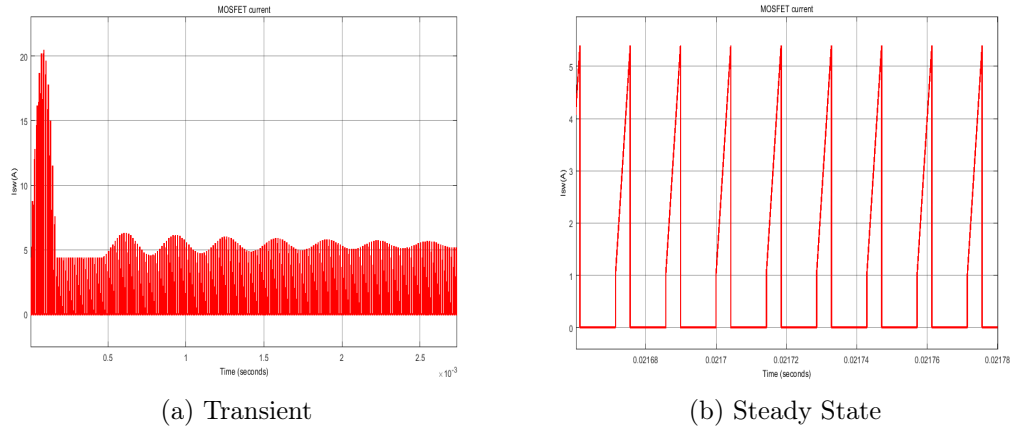
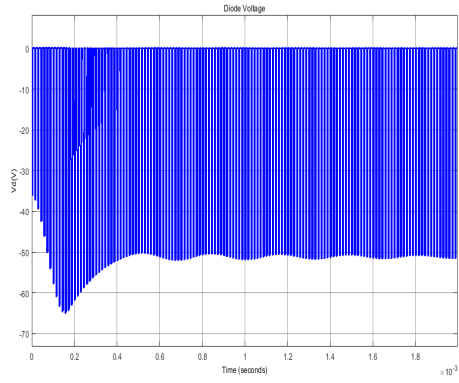


Figure 5.16: MOSFET Current at Transient and Steady State for  $V_{in} = 48\text{ V}$

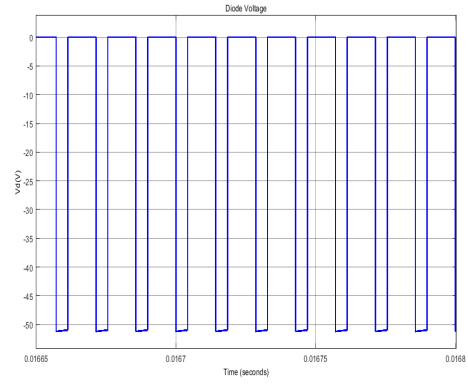
The maximum current that flows at switch is approximately 20 Amps as observed in Figure 5.16.

The voltage waveforms of diode when the maximum input voltage is applied are given in Figure 5.17. As can be seen, the maximum breakdown voltage at transient is approximately -70 Volts which is compatible with the analytical calculations.

The diode current at transient and steady state are given in Figure 5.18.

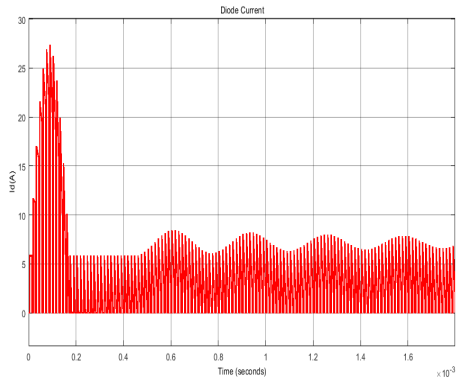


(a) Transient

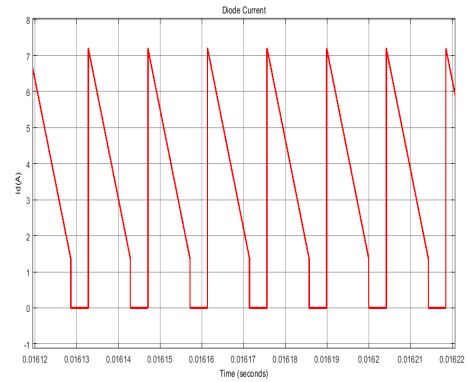


(b) Steady State

Figure 5.17: Diode Voltage for  $V_{in} = 48\text{ V}$



(a) Transient



(b) Steady State

Figure 5.18: Diode Current for  $V_{in} = 48\text{ V}$

The maximum current that flows on the diode is roughly 28 Amps.

## 5.2 Simulation in LTspice

### 5.2.1 Controller Implementation

The controller options are narrowed down to UC3842, LT1242, and LT3748. UC3842 and LT1242 are equivalent of each other. LT3748 has a simpler control loop and doesn't require a third winding whereas UC3842/LT1242 require a third winding to feed the controller and they have much complex feedback loop. However, the secondary side regulation of UC3842/LT1242 results in a more robust and stable system. Moreover, LT3748 can't be found in Turkey stock. Thus, UC3842/LT1242 are chosen as controller. Controller in the simulation is chosen as LT1242. Since UC3842 and LT1242 are equivalent of each other. The circuit schematic is given in Figure 5.19.

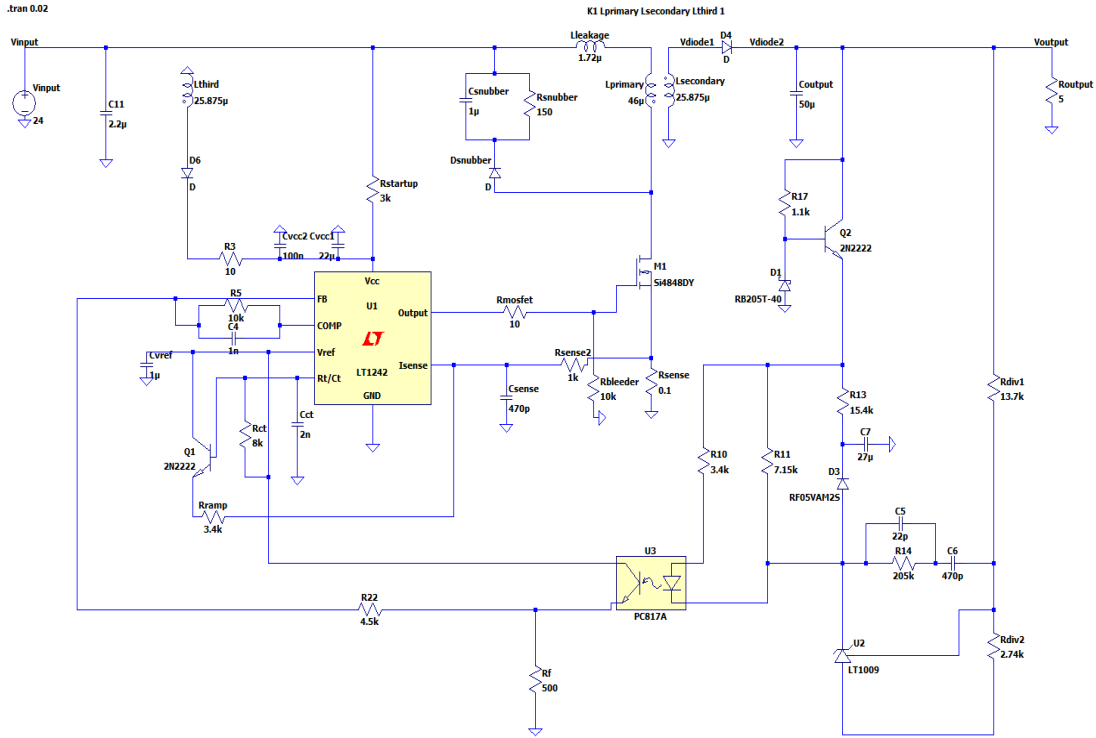


Figure 5.19: Flyback Converter Circuit Schematic with Controller in LTspice

For constructing the circuit, WeBench test environment of TI [2] and the application notes of LT1242, UC3842 and UC2842 are used [3]. The transformer parameters are revised after the test results. Detailed information about the sub-parts is explained below.

- Snubber Circuit

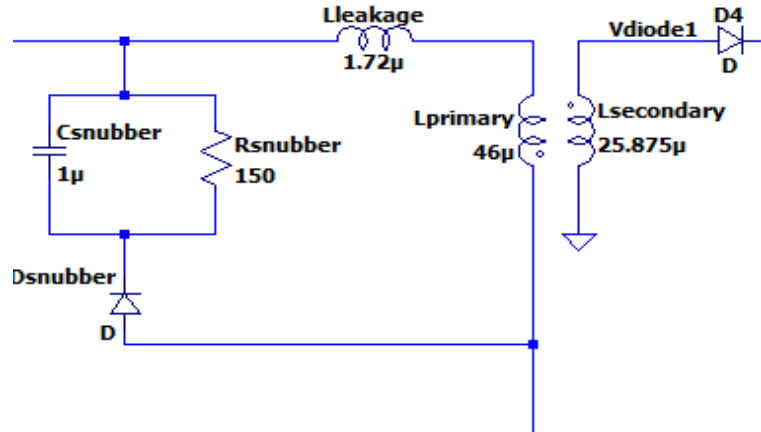


Figure 5.20: Snubber Circuit in LTspice

- Vcc

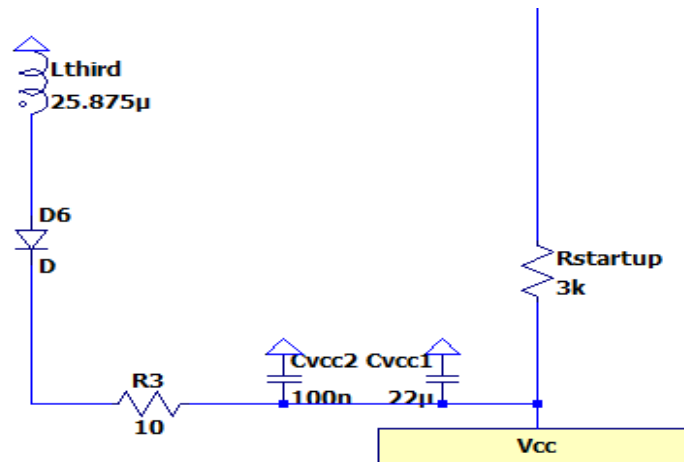


Figure 5.21: Power Delivery to Vcc

A third winding is wound up to the transformer in order to feed the controller in the steady state operation. This winding has the same turn number as the secondary winding and it delivers power to the controller. The  $R_{vcc1}$  and  $R_{vcc2}$  are used for filtering deviations in the  $V_{cc}$  voltage.  $R_{vcc2}$  is a small ceramic or film capacitor that is used for decreasing ESR value of the large capacitor.  $R_{startup}$  resistance is used in delivering power during start up, when the winding cannot generate enough voltage. It increases the source impedance. The value of  $R_{startup}$  is chosen smaller than the regular applications (100 k $\Omega$  in regular) since the input voltage is smaller than regular applications. (48 V max in our design).

- Vref

$V_{ref}$  generates 5 V constant output when  $V_{cc}$  is higher than the threshold voltage (12V for UC3842-LT1242). This pin is used in more than one subpart as voltage reference. To reduce the effect on voltage deviations in  $V_{cc}$  on the  $V_{ref}$  voltage, a large capacitor ( $1 \mu F$ ) is used as filter.

- Isense

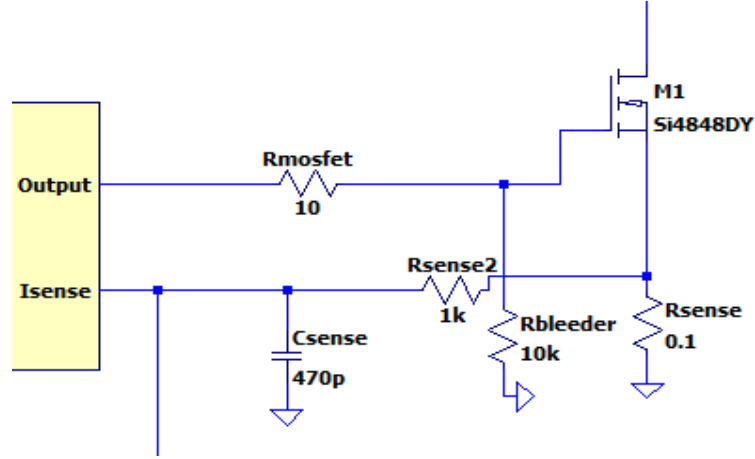


Figure 5.22: Current Sense in LTspice

$I_{sense}$  pin measures the input current via the voltage drop on the  $R_{sense}$  resistor.  $R_{sense}$  is chosen as  $0.1 \Omega$  to set current 10 A by the equation below:

$$I_{sense} = \frac{V_{Isense}}{R_{cs}}$$

The  $R_{bleeder}$  is placed to prevent the unwanted MOSFET turn-on due to leakage currents.  $R_{sense2}$  and  $C_{sense}$  construct a small RC filter and it is used to suppress switch transients.



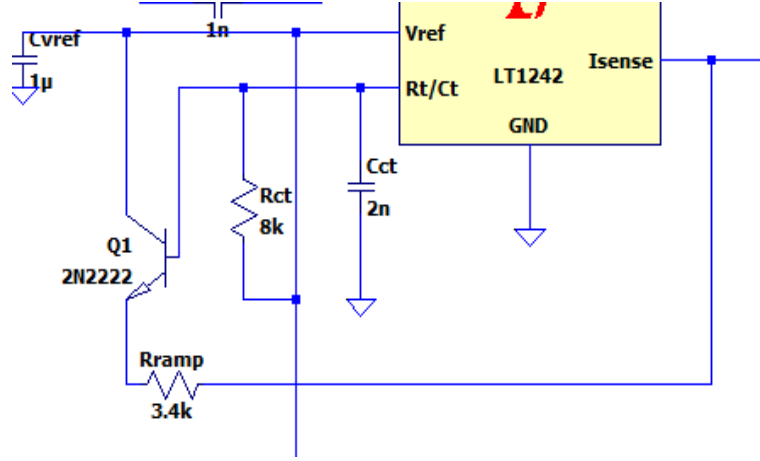


Figure 5.23: Oscillator Ramp Generator in LTspice

A ramp signal is generated by using the Q1 transistor and the  $C_{ct}$  (frequency set capacitor) in order to compensate the slope of the  $R_{sense}$  voltage. A fraction of this ramp signal is summed up with the feedback voltage via  $R_{ramp}$  resistor.

- $\frac{R_c}{R_t}$

The  $R_{rt}$  (frequency set resistor) and  $C_{ct}$  (frequency capacitor) is roughly set via the equation below. The capacitor value should be higher than 1 nF and the resistance should be higher than 5 k $\Omega$  according to the datasheet. After tuning the circuit in simulation, these values are chosen as  $R_{rt} = 8 \text{ k}\Omega$  and  $C_{ct} = 2 \text{ nF}$ . The oscillation frequency is determined as follows:

$$f_{osc} = \frac{1.72}{R_{rt} \cdot C_{ct}}$$

- Compensation Loop

The main aim of the compensation loop is to tune closed loop poles, zeros, gain and phase response in order to obtain a stable feedback loop. There are three main parts which are error amplifier of the controller, voltage regulator (TL431) and optocoupler.

– Voltage Regulator

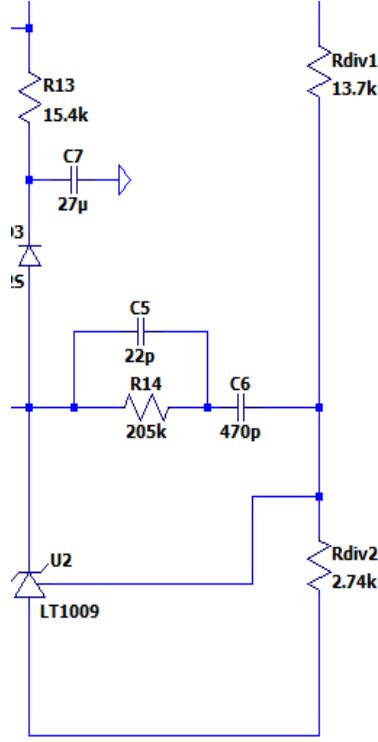


Figure 5.24: Voltage Regulator

The voltage regulator on the secondary side is used the node voltage to approximately 2.5V. The TL431 is used as regulator due to its accuracy and internal Op-amp.  $R_{div1}$  and  $R_{div2}$  are selected according to the desired power consumption.  $R_{div1}$  ( $R_{fbu}$ ) is chosen as in the equation below where  $Ref_{TL431}$  is 2.5 V and  $I_{fb}$  is chosen as 0.9 mA.

$$R_{fbu} = \frac{V_{out} - Ref_{TL431}}{I_{fb_{ref}}}$$

$R_{div1}$  is chosen as 13.7 k $\Omega$ . Then,  $R_{div2}$  is chosen as 2.74 k $\Omega$  by the following equation.

$$R_{fbB} = \frac{Ref_{TL431}}{V_{out} - Ref_{TL431}}$$

$R_{14}$ ,  $C_5$  and  $C_6$  are chosen in order to place a compensator zero for improving the phase margin at bandwidth frequency.

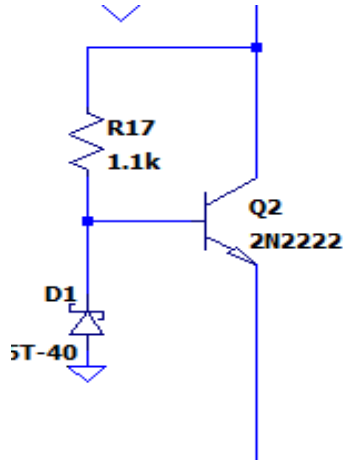


Figure 5.25: Cathode Current Circuit

The circuitry indicated in Figure 5.25 is responsible for providing sufficient cathode current to the TL431.

- Optocoupler

The optocoupler has a parasitic pole which is hard to characterize over frequency. So, by adding the  $R_f$ , we move this pole further away from the range of interest.

- Error Amplifier

The  $V_{comp}$  pin is the output of the error amplifier. The R5 and C4 that are connected to this pin is responsible for adding a compensation pole. R22 is added to the loop in order to increase the DC gain. This helps improving the bandwidth.

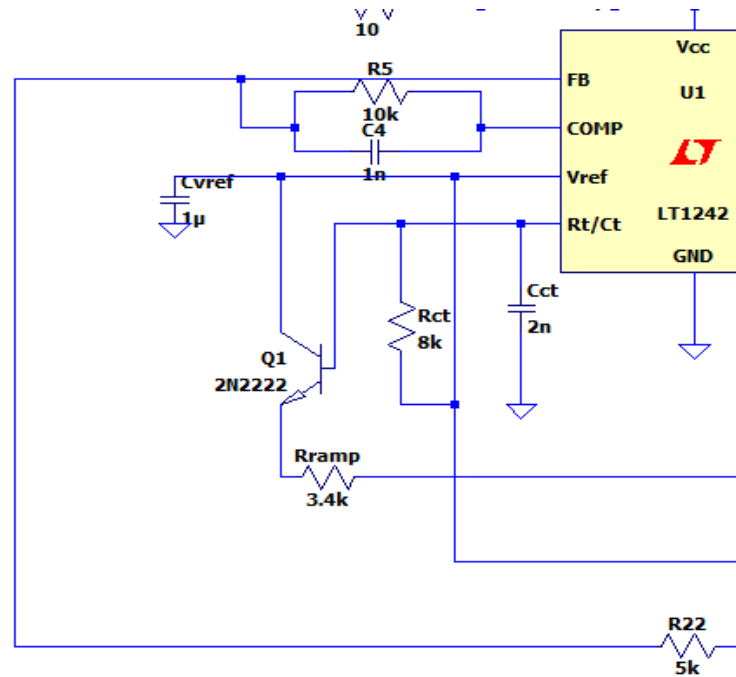


Figure 5.26: Error Amplifier in Compensation Loop

## 5.2.2 Simulation Results

The important characteristics of the circuit for 24V and 48V inputs are displayed below.

For minimum input voltage, 24 Volts, the output voltage waveforms is given in Figure 5.27.

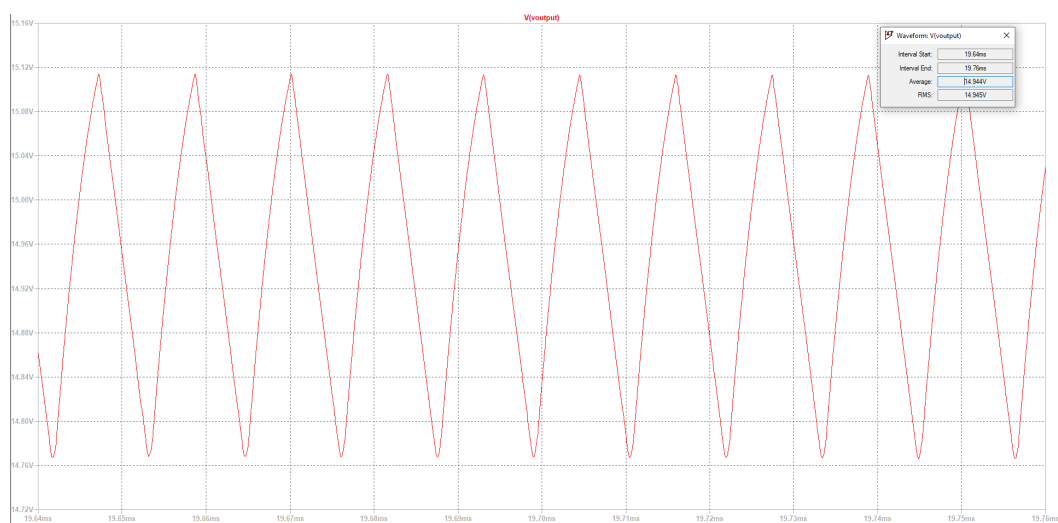


Figure 5.27: The Output Voltage Waveform for Minimum Input Voltage

It can be observed that the output voltage is approximately 14.95V and the voltage ripple is 0.34V which is satisfied for design considerations. The primary current waveform for minimum input voltage is given in Figure 5.28.

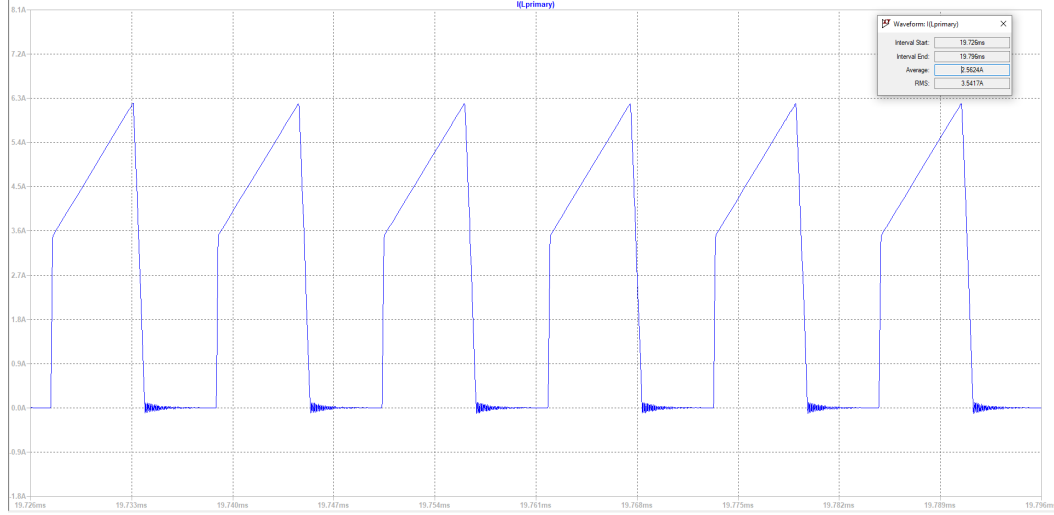


Figure 5.28: The Primary Current Waveform for Minimum Input Voltage

For primary cable, the minimum input voltage case is examined since it gives the maximum current. The RMS value of the primary current is 3.54A. Since the frequency is chosen as 70kHz, AWG25 cables are chosen to reduce skin effect. The cross-section of these cables are approximately  $0.16 \text{ mm}^2$ . Thus, 5 parallel cables are enough to make the average current density  $4 \text{ A/mm}^2$ .

The secondary current for minimum voltage case is given in Figure 5.29.

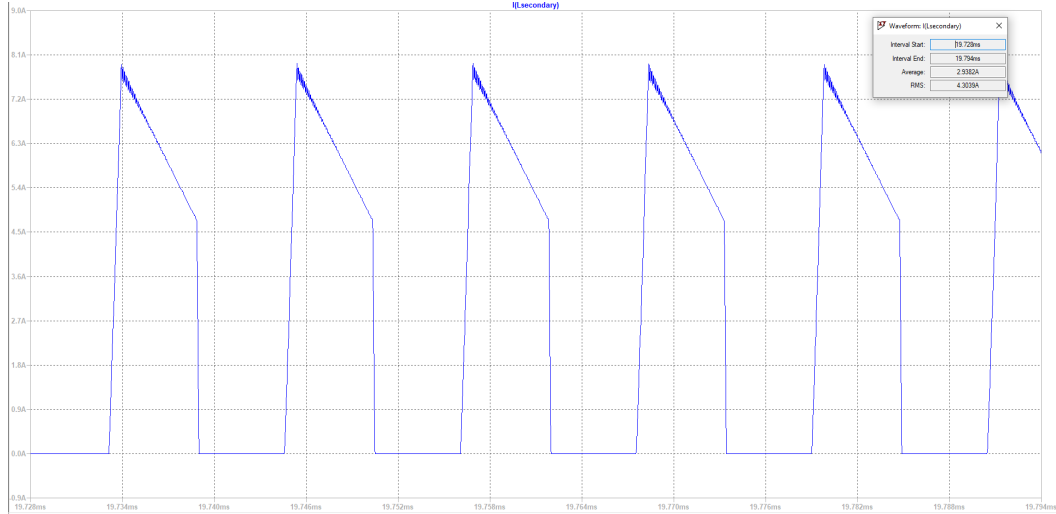


Figure 5.29: The Secondary Current Waveform for Minimum Input Voltage

The RMS value of the secondary current is 4.31 A. Thus, 7 parallel AWG cables are enough to make the average current density  $4 \text{ A/mm}^2$ .

The MOSFET voltage waveform in transient for minimum input voltage is given in Figure 5.30.

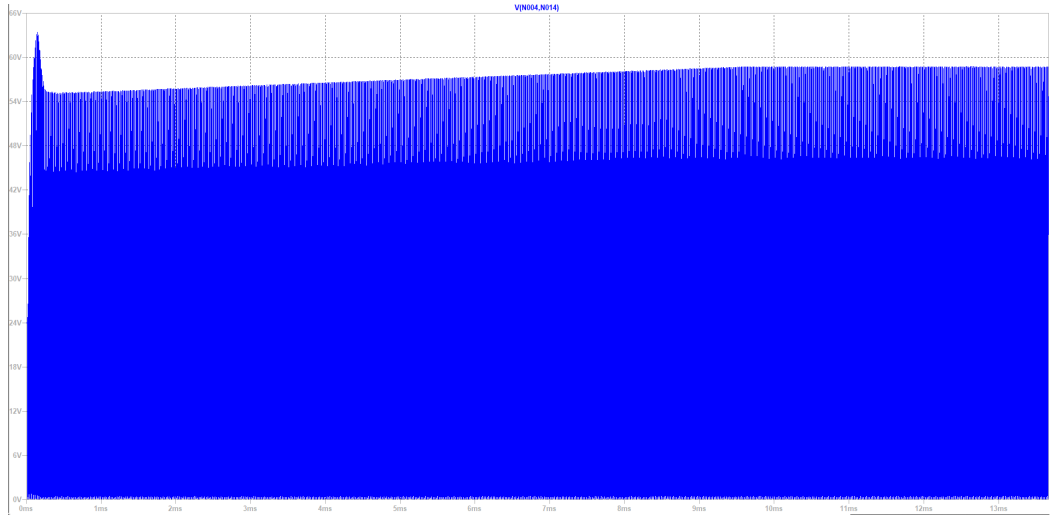


Figure 5.30: The MOSFET Voltage Waveform for Minimum Input Voltage in Transient

When the snubber is added to design, it is observed that the MOSFET voltage is reduced to 64V in transient state and 58V in steady state. Without the snubber, the MOSFET voltage reaches 300 V in transient state and 220 V in steady state due to leakage inductance. Therefore, the effect of the snubber circuit is observed easily. It is useful for reducing stresses on MOSFET.

The diode voltage waveform for minimum voltage is given Figure 5.31. It is observed that the maximum reverse voltage of diode 47 V with usage of snubber.

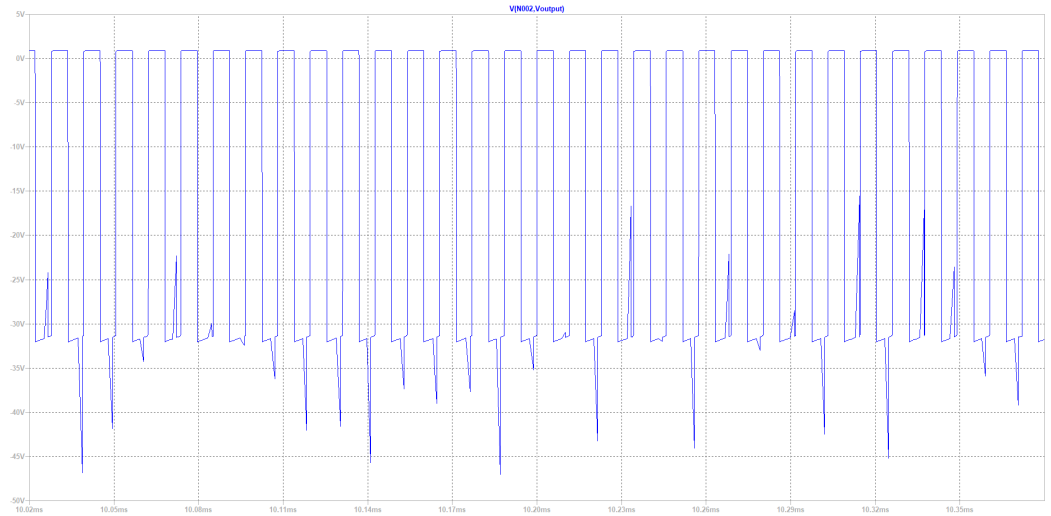


Figure 5.31: The Diode Voltage Waveform for Minimum Input Voltage in Steady State

For the maximum input voltage, 48 Volts, the important waveforms are given below. The output voltage waveform for maximum input voltage is applied is given in Figure 5.32. The output voltage is measured as 15.08V and the voltage ripple is 0.26V in steady state.

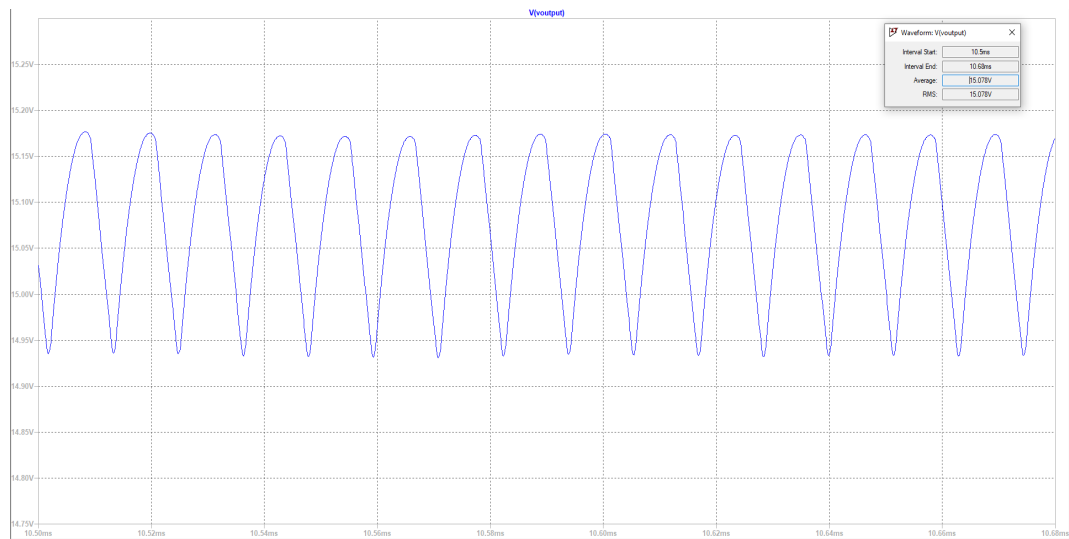


Figure 5.32: The Output Voltage Waveform for Maximum Input Voltage

The average power from average input current is measured from LTspice simulation tool, it can be seen in Figure 5.33.

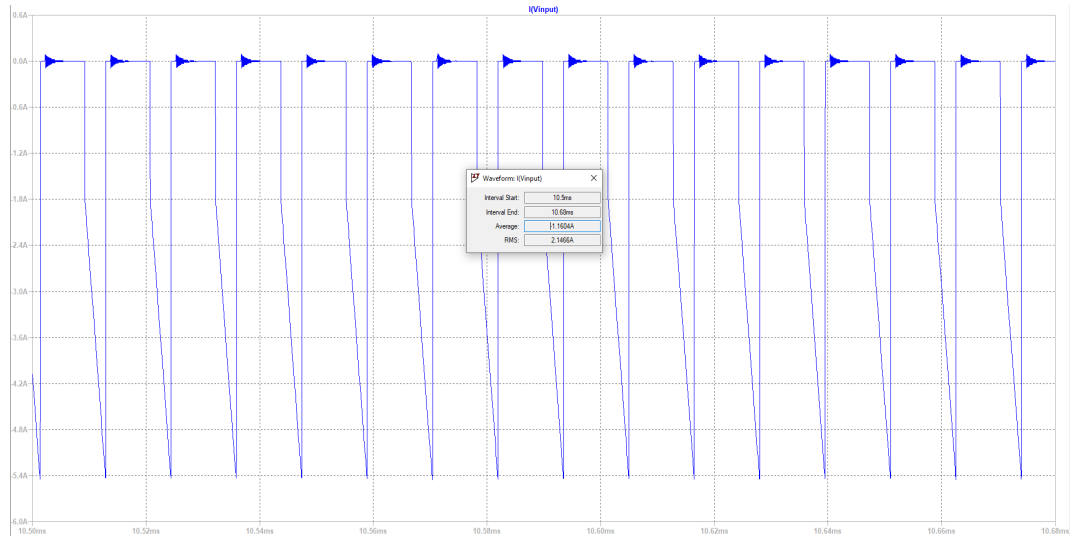


Figure 5.33: The Input Current Waveform for Maximum Input Voltage

By calculating the average power from the average input current, the efficiency is approximately 81.5%.



## Chapter 6

# Magnetic Design

The primary energy storage element of the flyback converter is magnetizing inductance. Therefore, design of the transformer is quite important for the application. While designing the transformer, the controller that selected should also be considered since, many controllers for converters are needed third winding in order to feed the controller in steady state.

### 6.1 Core Selection

According to analytical calculations, the minimum magnetizing inductance is calculated as  $31\mu H$ . In order to start to design transformer, the magnetizing inductance is determined as

$$L_m = 45\mu H$$

After deciding the magnetizing inductance, the peak currents of primary and secondary should be calculated in order to using cable selection and see the critical points for the transformer.

- at  $V_{in} = 24 V$

$$I_{in_{avg}} = \frac{45 W}{24 V} = 1.875 A$$

$$I_{pri_{avg}} = \frac{I_{in_{avg}}}{D} = \frac{1.875 A}{0.45} = 4.125 A$$

$$I_{Lm_{ripp}} = \frac{V_{in} D}{f_s L_m} = 3.26 A$$

$$I_{pri_{peak}} = I_{pri_{avg}} + \frac{I_{Lm_{ripp}}}{2} = 5.86 A$$

$$I_{sec_{peak}} = I_{pri_{peak}} N_{ps} = 7.81 A$$

- at  $V_{in} = 48 V$

$$I_{in_{avg}} = \frac{45 W}{48 V} = 0.9375 A$$

$$I_{pri_{avg}} = \frac{I_{in_{avg}}}{D} = \frac{0.9375 A}{0.29} = 3.23 A$$

$$I_{Lm_{ripp}} = \frac{V_{in} D}{f_s L_m} = 4.42 A$$

$$I_{pri_{peak}} = I_{pri_{avg}} + \frac{I_{Lm_{ripp}}}{2} = 5.44 A$$

$$I_{sec_{peak}} = I_{pri_{peak}} N_{ps} = 7.26 A$$

As can be observed from the calculation above, the peak values of primary and secondary don't change much when the input voltage changes.

After these calculations and many iterative attempts for selecting core, the desired core is selected as OP43434EC, the properties are shown in Table 6.1:

Component Model	Effective cross sectional area $A_e (mm^2)$	Maximum Magnetic Flux Density (T)	$A_L$ without the air-gap $\frac{nH}{n^2}$
OP43434EC	97.1	0.47 T	2933

Table 6.1: Core Properties

Since  $A_L$  value for this core is really high for this application, adding the air gap would be the solution for decrease the inductance. The air gap length is determined by choosing magnetic flux density value.

The magnetic flux density is chosen as  $B_{ac,max} = 0.2 T$  which is below the saturation point of the core that selected. The turns number of the transformer can be determined by using magnetic flux density:

$$B_{max} = \frac{N_p I_{pri_{peak}}}{R A_e} = \frac{N_p \cdot 5.86 A}{R \cdot 97.1 \cdot 10^{-6} m^2} = 0.2 T \text{ when } V_{in} = 24 V$$

$$\frac{N_p}{R} = N_p \cdot A_L = 3314 \cdot 10^{-9}$$

$$N_p = \sqrt{\frac{L_m}{A_L}}$$

Hence,

$$N_p = 12 \ \& \ A_L = 300 nH/T^2 \ \& \ N_s = 9$$

In order to reach desired  $A_L$  value, the air gap must be added. The length of the air gap can be determined as follows:

$$\begin{aligned}
R_{new} &= R_{core} + R_{gap} \\
\frac{1}{A_{L_{new}}} &= \frac{1}{A_{L_{core}}} + \frac{1}{A_{L_{gap}}} \\
\frac{1}{300 \cdot 10^{-9}} - \frac{1}{2933 \cdot 10^{-9}} &= R_{gap} \\
R_{gap} &= 3 \cdot 10^6 \text{ H}^{-1} \\
R_{gap} &= \frac{l_{gap}}{\mu_0 A_e} \\
l_{gap} &= 0.36 \text{ mm}
\end{aligned}$$

Therefore, the turn numbers of primary and secondary windings are 12 and 9, respectively. Also, the air gap length is determined as 0.36 mm

## 6.2 Cable Selection

The proper cable should be selected considering primary and secondary current RMS values, cross-section of the cable and switching frequency. The RMS values of primary and secondary windings can be calculated as:

$$I_{pri_{rms}} = 2.955 \text{ A}$$

$$I_{sec_{rms}} = 4.28 \text{ A}$$

The current density is assumed as  $J_{rms} = 3.5 \text{ A/mm}^2$ . Therefore, the cross-sectional area for the cables is calculated as:

$$A_{pri} = 0.84 \text{ mm}^2 \text{ \& } A_{sec} = 1.22 \text{ mm}^2$$

From AWG Cable Chart, AWG 25 is chosen for both primary and secondary windings. We have decided to use 5 parallel connected 25 AWG instead of one AWG copper for primary, and 7 parallel connected 25 AWG cable instead of one copper cable. Since cables with a larger cross-section have a smaller maximum frequency for %100 skin depth, we have decided to multiple cables that have enough maximum frequency for %100 skin depth instead of one cable. The maximum frequency for %100 skin depths is 85kHz for 26 AWG. This selection makes AC and DC resistances the same since we operate with %100 skin depth. Hence, the primary and secondary

windings cross-sections are calculated as follows:

$$A_{copper_{pri}} = 5 \cdot 25 \text{ AWG} = 5 \cdot 0.168 \text{ mm}^2 = 0.84 \text{ mm}^2$$

$$A_{copper_{sec}} = 7 \cdot 25 \text{ AWG} = 7 \cdot 0.168 \text{ mm}^2 = 1.176 \text{ mm}^2$$

In order to be sure about the selection, the fill factor should be checked from ratio of total cross-section area to the window area. The window area can be calculated from datasheet of the core:

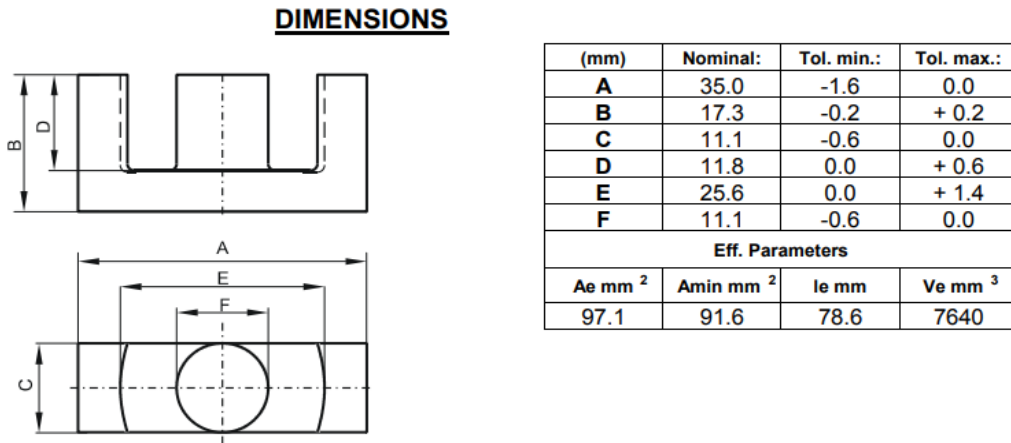


Figure 6.1: Dimensions of Selected Core

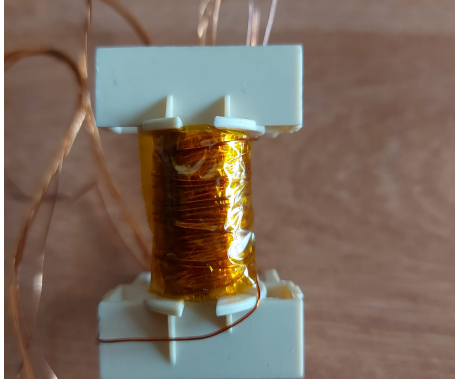
$$A_{window} = (E - C) \cdot D = (25.6 - 11.1) \cdot 11.8 = 85.55 \text{ mm}^2$$

Therefore, the fill factor can be calculated as:

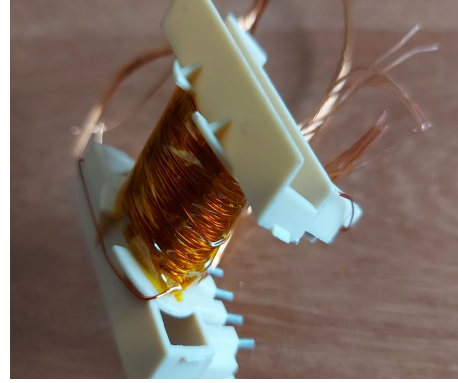
$$k_{cu} = \frac{N_{pri} \cdot A_{copper_{pri}} + N_{sec} \cdot A_{copper_{sec}}}{A_{window}} = \frac{12 \cdot 0.84 + 9 \cdot 1.176}{85.55} = 0.242$$

The fill factor is generally assumed as 0.3, so 0.242 is not a bad fill factor for this applications.

By using these design considerations and calculations, the transformer that we constructed is given in Figure 6.2.



(a)



(b)

Figure 6.2: Implementation of Transformer

By using LC meter, the magnetizing inductance or primary inductance and leakage inductance is measured as follows:



(a) Magnetizing Inductance



(b) Leakage Inductance

Figure 6.3: Measurement of Transformer

As can be seen from Figure 6.3, the magnetizing inductance is measured as expected. And the leakage inductance is relatively low.

## Chapter 7

# Component Selection

### 7.1 MOSFET Selection

As discussed in simulation chapter, the maximum voltage and current that seen from the MOSFET, is important while selecting the switch. At full load, MOSFET sees approximately 70 Volts in steady state. However, the maximum voltage in transient is nearly 100 Volts which compatible with the analytical calculation. Moreover, the maximum current that MOSFET sees at full load roughly 23 Amps. The Simulink simulations are made without snubber circuit which is require for According to these information P22F10SN Power MOSFET is selected. In addition to that, there will a snubber circuit in order to reset leakage inductance Therefore, it is considered too in LTspice simulations and it is observed that the maximum voltage is 64 Volts with using snubber circuit. Therefore, the selected MOSFET in Table 7.1 would works for this application. It has stock in özdisan.com.

Component	Model	$V_{ds}$	$I_d$	$R_{ds}$
MOSFET	P22F10SN	100 V	22 A	0.022 m $\Omega$

Table 7.1: The MOSFET Properties

### 7.2 Diode Selection

In order to select proper diode for this application the same manner can be applied with MOSFET selection. At the full load, the diode voltage drops down at approximately -70 Volts in transient. The maximum current in transient is roughly 25 Amps. These results are similar with analytical calculation. However, the simulation in LTspice with snubber circuit should be also considered. According to ideal simulation results MBR2580CT Schottky diode is selected first. The properties of this diode is given in Table 7.2.

Component	Model	$V_r$	$I_{forward}$
Diode	MBR2580CT	80 V	25 A

Table 7.2: Diode Properties

### 7.3 Output Capacitor Selection

The required output capacitance calculation is discussed in analytically calculation chapter. The required capacitance is found as  $50 \mu F$  and the output ripple is about 0.4 Volts which is satisfied the ripple condition. At the full load, the output current reaches above 8 Amps, the selected capacitor should have higher current rating than this value. From the components in laboratory, the available and suitable capacitor will be chosen.

### 7.4 Controller Selection

The controller options are narrowed down to UC3842, LT1242, and LT3748. UC3842 and LT1242 are equivalent of each other. LT3748 has a simpler control loop and doesn't require a third winding whereas UC3842/LT1242 require a third winding to feed the controller and they have much complex feedback loop. However, the secondary side regulation of UC3842/LT1242 results in a more robust and stable system. Moreover, LT3748 can't be found in Turkey stock. Thus, UC3842/LT1242 are chosen as controller.

### 7.5 RCD Snubber Circuit Selection

RCD Snubber circuit for flyback converter is needed for control the effects of leakage inductance in transformer and improve the reliability of power supply. After the switch is turn-off, the oscillations occur with the leakage inductance and the output capacitance. During these oscillations, the energy dissipates at the leakage inductance and it could be dangerous for the circuit. Therefore, the aim of the snubber circuit is reduce this effect. The circuit schematic of flyback converter with snubber circuit is given in Figure 7.1.

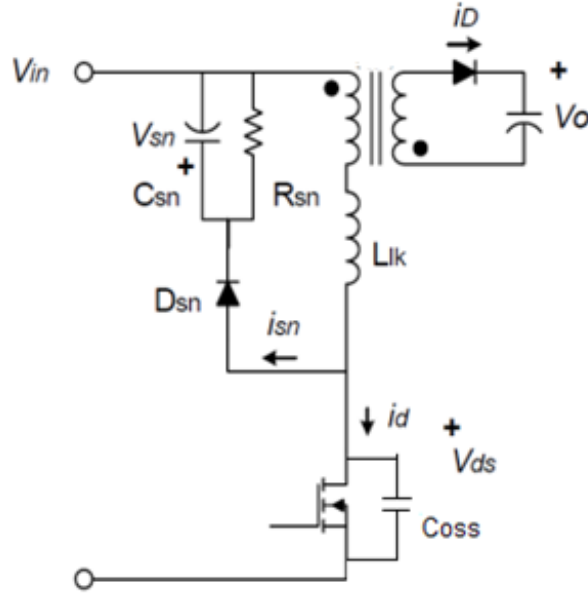


Figure 7.1: The Flyback Converter with Snubber Circuit

As the voltage across the snubber capacitor is called as  $V_{sn}$ , what it's aim is actually acting a voltage source and preventing the voltage on this switch from rising above  $V_{sn} + V_{in}$ . Overall, the energy stored in the leakage inductance flows through the diode right at some point and flows back into the capacitor. At the point, it was noticed that the snubber capacitor should be large enough so that even by this inductance interaction, its voltage stays constant near  $V_{sn}$  [4].

The average current on the snubber capacitor,  $C_{sn}$  should be zero for steady state as its average voltage is desired to be roughly constant.

$$i_{C_{sn}} = i_{diodeT_s} - \frac{V_{sn}}{R_{sn}}$$

In order to find the average diode current:



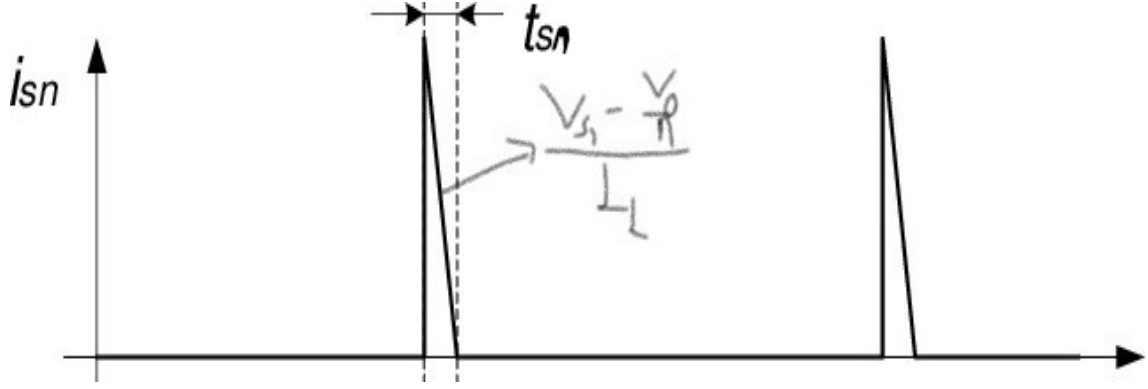


Figure 7.2: Diode Current in Snubber Circuit Time over a Full Period

At this stage an approximation can be made for the peak current. It is assumed that the leakage peak current is accepted in a fully-charged mode. So for CCM operation:

$$i_{peak} = I_{Lm} + \Delta i_{Lm}$$

The slope of the snubber current above Figure 7.2 can be found as well since the snubber is activated the voltage applied to the leakage inductance becomes.

$$\frac{V_{sn} - \frac{V_o}{n}}{L_{leakage}}$$

So the average snubber charge  $\Delta Q_{sn}$ , becomes the triangular area:  $\Delta Q_{sn} = \frac{1}{2} t_{sn} i_{peak}$   $t_{sn}$  is the time it takes for the current to be fully discharged. By using slope ratio,

$$i_{peak} = \frac{V_{sn} - \frac{V_o}{n}}{L_{leakage}} t_{sn} \rightarrow t_{sn} = \frac{i_{peak} L_{leakage}}{V_{sn} - \frac{V_o}{n}}$$

Inserting this  $t_{sn}$  and knowing also that  $i_{D_{sn}} = \frac{\Delta Q_{sn}}{t_{sn}} = \Delta Q_{sn} f_{sw}$  we obtain that:

$$i_{D_{sn}} = \frac{1}{2} i_{peak}^2 L_{leakage} f_{sw} \frac{1}{V_{sn} - \frac{V_o}{n}}$$

Also knowing  $i_{C_{sn}} = i_{diode_{Ts}} - \frac{V_{sn}}{R_{sn}}$ :

$$i_{peak}^2 L_{leakage} f_{sw} \frac{1}{V_{sn} - \frac{V_o}{n}} = \frac{V_{sn}}{R_{sn}}$$

$V_{sn}$  is a chosen as 30 V-35 V, meaning that the voltage level the switch should be able to be exposed is considered while choosing  $V_{sn}$ .

By solving the last equation for  $R_{sn}$  while measuring in LTspice that  $i_{peak} = 5.4 A$

at leakage:

$$R_{sn} = \frac{V_{sn}(V_{sn} - \frac{V_o}{n})}{i_{peak}^2 L_{leakage} f_{sw}} = \frac{35V \cdot (35V - (\frac{15V}{\frac{12}{9}}))}{5.4 A^2 \cdot 1.73 \mu H \cdot 70 kHz} \cong 148.7 \Omega \approx 150 \Omega$$

For the snubber capacitance,  $C_{sn}$ ,

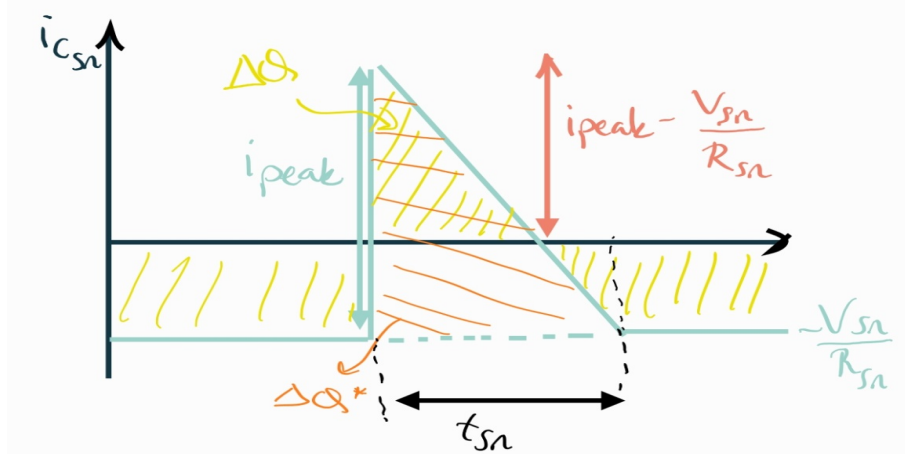


Figure 7.3: Calculation of Snubber Capacitance

For every period, when the snubber diode is on, the current is increased to charge the capacitor, then eventually being equal to the diode current. When the diode is off, it is equal to the current that passes through the snubber resistor as magnitude. Overall, a triangle occurs for each cycle. The larger triangle area is equal to  $\Delta Q^* = \frac{1}{2} i_{peak} t_{sn}$ .

And smaller triangle area similarly becomes by triangle ratio:

$$\frac{(i_{peak} - \frac{V_{sn}}{R_{sn}})^2}{i_{peak}} \Delta Q^* = \frac{(i_{peak} - \frac{V_{sn}}{R_{sn}})^2}{i_{peak}} \frac{1}{2} i_{peak} t_{sn}$$

By assuming either snubber time  $t_{sn}$  or  $\frac{V_{sn}}{R_{sn}}$  is small enough. Then we can get that:

$$\Delta Q = \frac{1}{2} i_{peak} t_{sn} \text{ or } \Delta Q = \frac{V_{sn}}{R_{sn}} (T_s - t_{sn})$$

Since  $\Delta Q = C \cdot \Delta V$

$$C_{sn} = \frac{\Delta Q}{\Delta V_{sn}} = \frac{\frac{V_{sn}}{R_{sn}} (T_s - t_{sn})}{\Delta V_{sn}}$$

Selecting the ripple rating as 7% and measuring oscillation duration approximately as 4  $\mu$ sec,

$$C_{sn} = \frac{\frac{35V}{150\Omega}(\frac{1}{70kHz} - 4\mu sec)}{35V \cdot 0.07} = \frac{2.4 \cdot 10^{-6}}{2.45V} \approx 1\mu F$$

Therefore, the RCD snubber circuit components are selected as:

- $V_{sn} = 30 - 35 V$
- $R_{sn} = 150 \Omega$
- $C_{sn} = 1\mu F$

## Chapter 8

# Conclusion

In this phase of the METU EE464 Hardware Project, at first among the suitable DC/DC Power Supplies according to given conditions and limitations, the advantages and disadvantages were compared. Considering the flexibility for magnetic and electrical design, the flyback converter was chosen to be implemented. After deciding on its operation mode, the necessary parameters to simulate the circuit were calculated by relying on given theoretical knowledge this year. By considering the input range, the circuit simulation results were obtained in Simulink software as applying the calculated parameters. During the implementation of this stage, the magnetic design for the transformer of the circuit was also considered and planned simultaneously due to restrictions in the market. Analyzing that the results were consistent with given conditions, the transformer design was performed in the laboratory. After that the inductance values belong to transformer were measured to verify that the values obtained under real conditions were also consistent and they did not violate the given operation conditions and boundaries. Besides these stages, LTSpice simulations were also performed by taking into the controller implementation. Due to stock issues in Turkish market, the suitable controller choices were listed. After selecting one of the suitable ones, RCD Snubber circuit was designed and added to the circuit to balance the oscillations. With all these, it was observed that the given conditions were also satisfied in this software as well.

# References

- [1] T. Instruments, *Lm34xx how to design flyback converter with ... - ti.com*, 2016. [Online]. Available: <https://www.ti.com/lit/an/snva761a/snva761a.pdf>.
- [2] *Webench® power designer*. [Online]. Available: <https://www.ti.com/design-resources/design-tools-simulation/webench-power-designer.html>.
- [3] —, *Ucx84x current-mode pwm controllers - texas instruments*, Apr. 1997. [Online]. Available: <https://www.ti.com/lit/ds/symlink/uc3842.pdf>.
- [4] T. McRae, *Lecture 8.7: The flyback converter 4 (rcd snubber)*, Dec. 2020. [Online]. Available: <https://www.youtube.com/watch?v=WQt03i5ZG74>.